

Synthesis, Structure, and DNA Binding Studies of Copper(II) Complexes of Terpyridine Derivatives

V. Uma, V. G. Vaidyanathan, and Balachandran Unni Nair*

Chemical Laboratory, Central Leather Research Institute, Adyar, Chennai 600 020 Tamil Nadu, India

Received October 4, 2004; E-mail: nairbu@rediffmail.com

Two copper(II) complexes, $Cu(ttpy)_2^{2+}$ **1** and $Cu(Brphtpy)_2^{2+}$ **2**, were synthesized and characterized for their DNA binding and cleaving ability. The crystal structure of complex **1** reveals an axially compressed six-coordinate geometry around Cu(II). In spite of having an axially compressed geometry, the polycrystalline EPR spectrum of complex **1** at 298 K shows $g_{\parallel} > g_{\perp}$, indicating a $d_{x^2-y^2}$ ground state for the Cu(II) complex. Both complexes **1** and **2** bind to CT DNA intercalatively with moderate binding strength ($K_b = (8.4 \pm 0.2) \times 10^3$ and $(10.9 \pm 0.2) \times 10^4$ M^{-1} (1 M = mol dm^{-3}) respectively). Both of these complexes cleave plasmid DNA efficiently in the presence of peroxide.

Recent years have seen tremendous interest in studies related to the interaction of transition metal ions with nucleic acid because of their relevance in the development of new reagents for biotechnology and medicine. These studies are also important to understand the toxicity of drugs containing metal ions.[1–4] There has also been substantial interest in the rational design of novel transition metal complexes, which bind and cleave duplex DNA with high sequence and structure selectivity.[5–10] Endonucleases rapidly hydrolyze DNA at neutral pH and physiological temperature. It is more challenging to synthesize small molecule catalysts capable of mimicking the function of these endonucleases. A number of oxidative cleavage reagents have been utilized with great success for DNA footprinting, for locating base mismatches and loop regions, for locating conformation variations in DNA and as chemotherauptic agents.[11–20] The metal ion, which has been most widely exploited for this purpose, is copper(II).[21–26] Copper is a bio-essential element with two relevant oxidation states, +1 and +2. Coordination complexes of copper have been extensively used in metal ion-mediated DNA cleavage through the generation of hydrogen abstracting activated oxygen species.[27] The most widely exploited oxidative cleavage agent is the bis(1,10-phenanthroline) copper(I) cation.[28–30] In the presence of H_2O_2 or O_2 plus a reducing agent, this chelate effectively cleaves B-DNA in the minor groove. Numerous other ligands have also been complexed with copper ion, to promote the oxidative degradation of DNA. These ligands include tambjamine, *o*-quinacridines, clip-phen, 2,2′-bipyridine, tripeptide gly–gly–his, and various hydroxamic acids.[31–36] Many of them also show the capability of RNA scission via phosphoester transesterification.[37] DNA footprinting agents, on the other hand, should bind and cleave DNA non-selectively. It is also important that its binding to DNA should be relatively weak. In this communication we describe the synthesis, structure, and metallonuclease activity of copper(II) complexes of two terpyridyl derivatives, viz., tolyl terpyridyl (a) and bromophenylterpyridyl (b) (Chart 1).

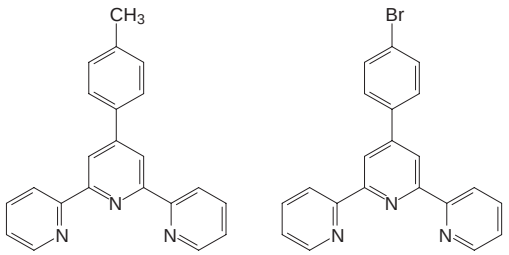

Chart 1.

Experimental

Chemicals. 2-Acetyl pyridine, 4-bromobenzaldehyde, and *p*-tolualdehyde were obtained from Sigma Aldrich, USA and used as received. Hepes and Tris were obtained from SRL chemicals, Mumbai. Calf Thymus DNA (CT DNA) was obtained from Fluka chemicals. All chemicals and reagents used were of analytical grade received from Ranbaxy, Mumbai. A stock solution of DNA was prepared by stirring a sample dissolved in 10 mM Hepes buffer (pH 7.2) at 4 °C. The solution was dialyzed exhaustively against Hepes buffer for 48 h. and filtered using a membrane filter obtained from Sartorius (0.45 μm). The filtered DNA solution in the buffer gave a UV absorbance ratio (A_{260}/A_{280}) of about 1.8–1.9, indicating that the DNA was sufficiently free from protein.[38] The concentration of DNA was determined using an extinction coefficient of 6600 $M^{-1}\,cm^{-1}$ at 260 nm.[39] All of the experiments were carried out in Tris buffer at pH 7.2 in Milli Q triply deionized water.

Physical Measurements. UV–visible spectra of the complex and DNA binding studies were recorded on a Perkin-Elmer Lambda 35 double beam spectrophotometer at 25 °C. The solid state absorption spectra of the complexes were recorded using a Perkin-Elmer Lambda 35 double-beam spectrophotometer with a Labsphere reflectance accessory. The emission spectra were recorded on a Hitachi 650-40 spectrofluorimeter. The FAB mass spectra

Published on the web May 6, 2005; DOI 10.1246/bcsj.78.845

were recorded on a JOEL SX 102/DA-6000 Mass spectrometer/Data System using Argon/Xenon (6 kV, 10 mA) as the FAB gas. The accelerating voltage was 10 kV and the spectra was recorded at room temperature in a *m*-nitrobenzyl alcohol (NBA) matrix. X-band electron paramagnetic resonance (EPR) spectra at room temperature and liquid-nitrogen temperatures were recorded on a Varian E-112 spectrometer, with 100 kHz field modulation of 0.5 mT; the microwave power of 10 mW and the *g* calibration were effected by diphenylpicrylhydrazyl (DPPH). Elemental analyses were performed using a Heraeus CHN-O-rapid analyzer.

Synthesis. $[Cu(ttpy)_2](ClO_4)_2$ (1): The ligand, ttpy was synthesized as per a reported procedure.[40] The complex was prepared in high yield from a reaction of $Cu(ClO_4)_2 \cdot 6H_2O$ (0.093 g, 0.25 mmol) in methanol (20 mL) with ttpy (0.162 g, 0.5 mmol) under reflux for 15 min. A greenish-blue solid, obtained upon cooling, was filtered and washed with diethyl ether and dried in vacuo over $CaCl_2$. The sample was recrystallized from acetonitrile. Anal. Calcd for $C_{44}H_{34}Cl_2N_6O_8Cu$: C, 58.12; H, 3.77; N, 9.24; Cu, 6.99%. Found: C, 58.02; H, 3.65; N, 9.29; Cu, 6.88%. UV–visible spectra [λ_{max} nm (ε, $M^{-1}\,cm^{-1}$)]: 277 (41460), 360 (3020), 572 (68), 680 (94) in DMSO. FAB MS, *m*/*z*: 709 $(ML_2 - 2(ClO_4) - H)^+$, 386 $(ML - 2(ClO_4) - H)^+$. The complex is soluble in DMSO and acetonitrile.

$[Cu(Brphtpy)_2]$ $(ClO_4)_2$ (2): The ligand Brphtpy was synthesized as per a reported procedure.[41] The complex was prepared in a similar way to that in the synthesis of **1** by reacting the metal salt and ligand in a molar ratio of 1:2. Anal. Calcd for $C_{42}H_{28}N_6Br_2Cl_2O_8Cu$: C, 48.55; H, 2.72; N, 8.09; Cu, 6.12%. Found: C, 48.42; H, 2.65; N, 8.11; Cu, 6.08%. UV–visible spectra [λ_{max} nm (ε, $M^{-1}\,cm^{-1}$)]: 278 (61970), 360 (6140), 574 (65), 641 (71) in DMSO. FAB-MS, *m*/*z*: 839 $(ML_2 - 2ClO_4 - H)^+$, 451 $(ML - 2ClO_4 - H)^+$. The complex is soluble in DMSO and sparingly soluble in acetonitrile and water.

DNA-Binding and Cleavage Experiments. The electronic spectra of Cu(II) complexes were monitored in both the absence and presence of DNA at around 278 nm. Absorption titration experiments were performed by maintaining the metal complex concentration constant (10 μM) and varying the nucleic acid concentration (0–250 μM). A reference cell contained DNA alone to nullify the absorbance due to the DNA at the measured wavelength. From the absorption titration data, the binding constant was determined using

$$[DNA]/(\varepsilon_a - \varepsilon_f) = [DNA]/(\varepsilon_b - \varepsilon_f) + 1/K_b(\varepsilon_b - \varepsilon_f), \quad (1)$$

where ε_a, ε_f, and ε_b correspond to $A_{obsd}/[Cu]$, the extinction coefficient for the free copper complex, and the extinction coefficient for the copper complex in the fully bound form, respectively. A plot of $[DNA]/(\varepsilon_a - \varepsilon_f)$ versus [DNA], gives K_b as the ratio of the slope to the intercept.

Viscometric experiments were carried out using an Ostwald-type viscometer of 2 mL capacity, thermostated in a water bath maintained at 25 ± 1 °C. The flow rates of the buffer (10 mM), DNA (200 μM), and DNA in the presence of Cu(II) complex at various concentrations (20–150 μM) were measured with a manually operated timer at least three times to agree within 0.2 s. The relative viscosity was calculated according to the relation $\eta = (t - t_0)/t_0$, where t_0 is the flow time for the buffer and t is the observed flow time for DNA in the presence and absence of the complex. A plot of $(\eta/\eta_0)^{1/3}$ versus $1/R$ (R = [DNA]/[Cu]) was constructed from viscosity measurements.[42]

The cleavage of plasmid DNA was monitored using agarose gel electrophoresis. Supercoiled pBR322 DNA (120 ng) in Tris buffer (50 mM, pH 7.5) with 50 mM NaCl was treated with the copper(II) complexes (75 μM) and H_2O_2 (125 μM and 500 μM). The samples were incubated for 1 h at 37 °C. A loading buffer containing 0.25% bromophenol blue, 40% (w/v) sucrose and 0.5 M EDTA was added and the electrophoresis of the DNA cleavage products was performed on 0.8% agarose gel containing 0.5 μg/mL ethidium bromide. The gels were run at 50 V for 3 h in TBE buffer and the bands were photographed by a gel documentation system.

EPR spin trapping was used for detecting a short-lived free radical intermediate. EPR spectra were recorded at a resonant frequency of 9.78 GHz using a Bruker EMX 6/1 spectrometer equipped with an ER 4103TM cavity. The spectrometer settings used for the experiments were as follows: microwave power, 2.0 mW; modulation frequency, 100 kHz; time constant, 5.12 ms; sweep time, 10.48 s; modulation amplitude, 1 G; number of data points, 1024. EPR spin trapping experiments were carried out using DMPO (200 mM); complex **1** (30 μM) and H_2O_2 (125 μM).

X-ray Crystallography of $[Cu(ttpy)_2](ClO_4)_2$. The diffraction intensities of an approximately $0.3 \times 0.2 \times 0.2$ mm^3 green rectangular plate crystal were collected at room temperature with graphite-monochromatized Mo Kα (0.71069 Å) radiation using an Enraf-Nonius CAD4 diffractometer. The unit-cell dimensions were determined from 25 well-centered reflections with $2.49 < \theta < 25.00$. The data were corrected for Lorentz and polarization effects, and an absorption correction was applied using psi-scan data. A summary of the crystal data is presented in Table 1. The structure was solved by a direct method and subsequent Fourier difference techniques (SIR92). The refinement of F^2 was carried out by full-matrix least squares techniques (SHELXL-97). Even though most of the hydrogen atoms were located from Fourier difference maps, they were included in the refinement at calculated positions (C–H 0.96 Å) riding on their respective parent atoms. All non-hydrogen atoms were refined with anisotropic thermal parameters, while the hydrogen atoms were refined with overall isotropic thermal parameters.

Crystallographic data were submitted with CCDC. Copies of this can be obtained free of charge from the Director, CCDC, 12 Union Road, Cambridge, CB2 1EZ UK (fax: +44-1223-336-033; e-mail: deposit@ccdc.cam.ac.uk or www.ccdc.cam.ac.uk) quoting the deposition number CCDC 218516 for complex **1**.

Table 1. Crystal Data for $[Cu(ttpy)_2](ClO_4)_2$

Empirical formula	$C_{44}H_{42}Cl_2CuN_6O_{12}$
Formula weight	981.28
Temperature	293(2) K
Wavelength	0.71069 Å
Crystal system, space group	Orthorhombic, *Fddd*
Unit cell dimensions	$a = 8.833(17)$ Å $\alpha = 90°$
	$b = 24.466(9)$ Å $\beta = 90°$
	$c = 48.805(17)$ Å $\gamma = 90°$
Volume	10547(21) $Å^3$
Z, Calculated density	8, 1.236 mg/m^3
Absorption coefficient	0.575 mm^{-1}
F(000)	4056
Crystal size	$0.3 \times 0.2 \times 0.2$ mm^3
Final *R* indices ($I > 2\sigma(I)$)	$R1 = 0.0593$, $wR2 = 0.1868$
R indices (all data)	$R1 = 0.0874$, $wR2 = 0.1938$
Extinction coefficient	0.00003(5)
Reflections collected/unique	4555/2330 [R(int) = 0.0402]

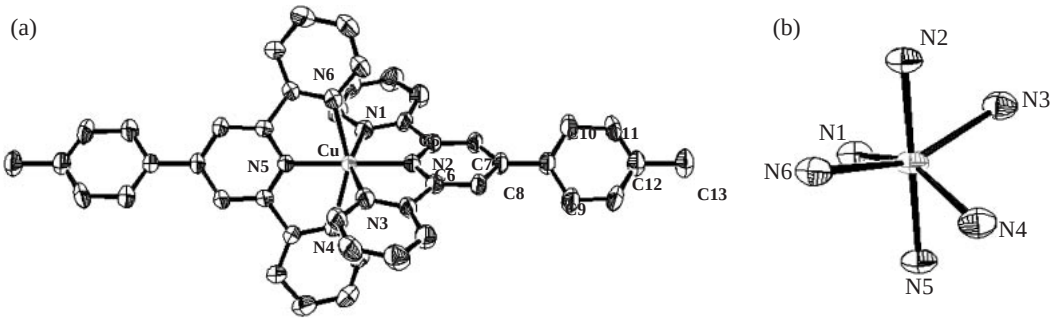

Fig. 1. (a) ORTEP diagram of $[Cu(ttpy)_2]^{2+}$. (b) Coordination around Cu^{2+}.

Table 2. Selected Bond Lengths (Å) and Bond Angles (°) for $Cu(ttpy)_2^{2+}$ (**1**)

Cu–N(2)	1.981 (5)
Cu–N(5)	1.981 (5)
Cu–N(1)	2.205 (4)
Cu–N(3)	2.205 (4)
Cu–N(4)	2.205 (4)
Cu–N(6)	2.205 (4)
N(2)–Cu–N(3)	77.21 (10)
N(5)–Cu–N(3)	102.79 (10)
N(5)–Cu–N(2)	180.00 (1)
C(4)–C(5)–C(6)	123.51 (4)
C(5)–C(6)–C(7)	123.51 (4)
C(7)–C(8)–C(9)	121.80 (3)
C(10)–C(9)–C(8)	120.72 (3)
C(11)–C(12)–C(13)	121.44 (3)
C(6)–C(5)–N(1)	115.11 (4)
N(2)–C(6)–C(5)	114.69 (4)

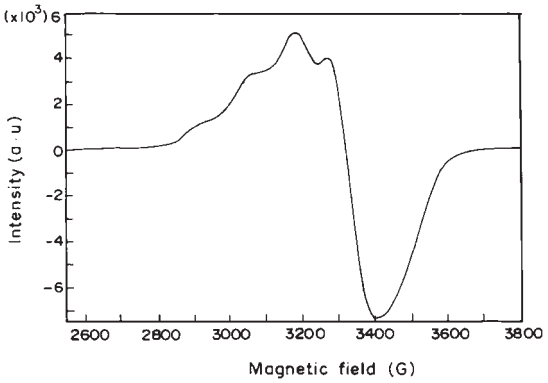

Fig. 2. Polycrystalline EPR spectrum of **1** at 298 K. (Microwave frequency = 9.81 GHz, power = 10 mW, modulation frequency = 100 kHz, modulation amplitude = 1.5 G.)

Results and Discussion

Synthesis and Crystal Structure. Complexes **1** and **2** were synthesized in high yield from the reaction of tolylterpyridyl and bromophenylterpyridyl with copper(II) perchlorate in a methanol medium. The authenticity of the complexes was ascertained from a FAB mass spectral analysis. The mass spectra of complexes **1** and **2** show $(ML_2 - 2ClO_4 - H)^+$ peaks at m/z 709 and 839, respectively, for the $Cu(ttpy)_2^{2+}$ and $Cu(Brphtpy)_2^{2+}$ cations. Complex **1**, for which a single crystal could be grown, crystallizes as orthorhombic crystals. The molecular structure of **1** is shown in Fig. 1. Complex **1** is a centrosymmetric cation. Even though a large majority of copper(II) complexes exhibiting a six-coordinate geometry have been known to show axial elongation with two longer Cu(II)–ligand bonds and four normal Cu(II)–ligand bonds, complex **1** behaves differently. The geometry of complex **1** is similar to that reported by Colbran et al. for their copper complex.[43] This six-coordinate copper(II) complex, **1** shows a tetragonal distortion due to the geometrical constraints of the tridentate ligand. The coordination around the metal ion is depicted in Fig. 1b. The two copper–nitrogen bonds, Cu–N(2) and Cu–N(5) can be considered as two axial bonds, the N(2)–Cu–N(5) bond angle being 180°. The tetragonal plane exhibits a considerable distortion with the N(3)–Cu–N(5) angle being 102.79° and the N(2)–Cu–N(3) angle being compressed to 77.21°. The two axial Cu–N bonds show the normal Cu–N bond length of 1.981 Å, whereas the other four Cu–N bonds are elongated with a bond length of 2.205 Å. The important bond lengths and bond angles for complex **1** are given in Table 2. It is pertinent to note that bis(diethylenetriamine) copper(II) cation, which also has a CuN_6 core, like complex **1**, has an elongated rhombic octahedral stereochemistry.[44] On the other hand, in the case of copper(II) complexes of meridonal tri-N-donor ligands, like 2,6-di(pyrazol-1-yl)pyridine, Jahn–Teller distortion has been reported to take the form of an elongated axis, which in the solid state is often dynamically disordered in the molecular xy plane.[45] Room-temperature X-ray diffraction studies reveal a tetragonal elongation for this copper(II) complex.

EPR and Electronic Spectra of the Complexes. Jahn–Teller distortion leading to axial compression gives rise to an EPR spectrum with $g_\perp > g_\parallel$.[46] The complex cation $Cu(terpy)_2^{2+}$, which has a compressed rhombic geometry, in fact exhibits an epr spectrum with $g_\perp > g_\parallel > g_e$ pattern.[47] However, complex **1** shows an inverted spectra. Polycrystalline EPR spectra of complex **1** at 298 K are shown in Fig. 2. The spectra clearly indicate a $g_\parallel > g_\perp$ pattern with $g_\parallel = 2.25$ and $g_\perp = 2.05$. Fluxionality in hexacoordinated copper(II) complexes with CuN_6 core has been commonly observed. Such fluxionality will certainly affect the "g" anisotropy. Hence, the EPR spectra of frozen solutions of complexes **1** and **2** were also examined at 77 K. Just like the 298 K spectrum, the 77 K spectrum is also an axial spectrum with $g_\parallel > g_\perp$, as shown in Fig. 3, indicative of the $d_{x^2-y^2}$ ground state. The EPR parame-

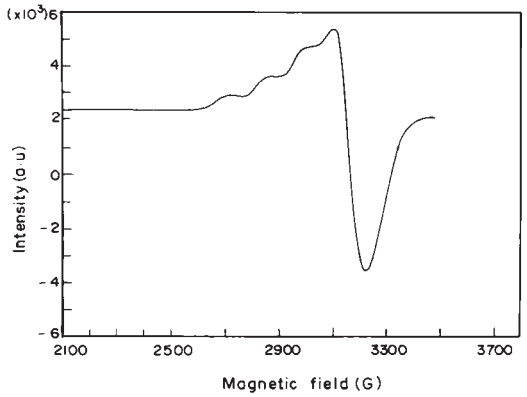

Fig. 3. EPR spectra of frozen solution of complex **1** at 77 K. (Microwave frequency = 9.23 GHz, power = 5 mW, modulation frequency = 100 kHz, modulation amplitude = 5 G.)

Table 3. EPR Spectral Parameters for Complexes **1** and **2** at 77 K

Complex **1**	$g_\perp = 2.007$; $g_\parallel = 2.151$; $A_\parallel = 145$ G
Complex **2**	$g_\perp = 2.006$; $g_\parallel = 2.143$; $A_\parallel = 135$ G

ters extracted from the 77 K spectra are given in Table 3. It is clear from Table 3 that both complexes **1** and **2** have almost identical $g_\parallel$, $g_\perp$, and $A_\parallel$ values, indicating a similar electronic environment for Cu(II) in both complexes. Hence, it is clear that the axial compression observed in complex **1** is unlikely to be due to any electronic effect. The axially compressed stereochemistry arises due to constraints imposed by the ligand.

The spectroscopic properties of copper(II) complexes are generally governed by Jahn–Teller coupling. The solid state absorption spectra of complexes **1** and **2** are shown in Figs. 4a and 4b. The spectra show a broad absorption band between 600–800 nm for both complexes. Because both **1** and **2** are six coordinate complexes, their solution spectra are not expected to be very different from the solid state spectra, since the solvent will not enter the coordination sphere of the metal ion. The electronic spectra of complexes **1** and **2** in DMSO are shown in Fig. 5. The spectrum is dominated by an intense transition around 278 nm, which is an intraligand transition. Ligand field transition has been observed as a broad envelop between 480 nm to 850 nm (inset of Fig. 5). Since the polycrystalline EPR of **1** suggests the presence of an odd electron in the $d_{x^2-y^2}$ orbital, one would expect $d_{xz,yz} \rightarrow d_{x^2-y^2}$, $d_{xy} \rightarrow d_{x^2-y^2}$, and $d_{z^2} \rightarrow d_{x^2-y^2}$ electronic transitions with one electron orbital sequence $d_{x^2-y^2} > d_{z^2} > d_{xy} > d_{xz,yz}$. Complex **1** shows ligand field transitions centered at 680 nm and 572 nm which can be assigned to $d_{xy} \rightarrow d_{x^2-y^2}$ and $d_{xz,yz} \rightarrow d_{x^2-y^2}$, respectively. The corresponding spectral bands for complex **2** have been observed at 641 nm and 574 nm. The third spectral band due to $d_{z^2} \rightarrow d_{x^2-y^2}$ is usually not observed in tetragonally distorted complexes because of their low intensity.[48] In the case of complex **2** however, the transition could be seen as a shoulder around 720 nm. In the case of complex **1**, the $d_{xy} \rightarrow d_{x^2-y^2}$ transition is very intense compared to the corresponding transition in complex **2**; as a result, the lowest energy $d_{z^2} \rightarrow d_{x^2-y^2}$ transition could not be resolved.

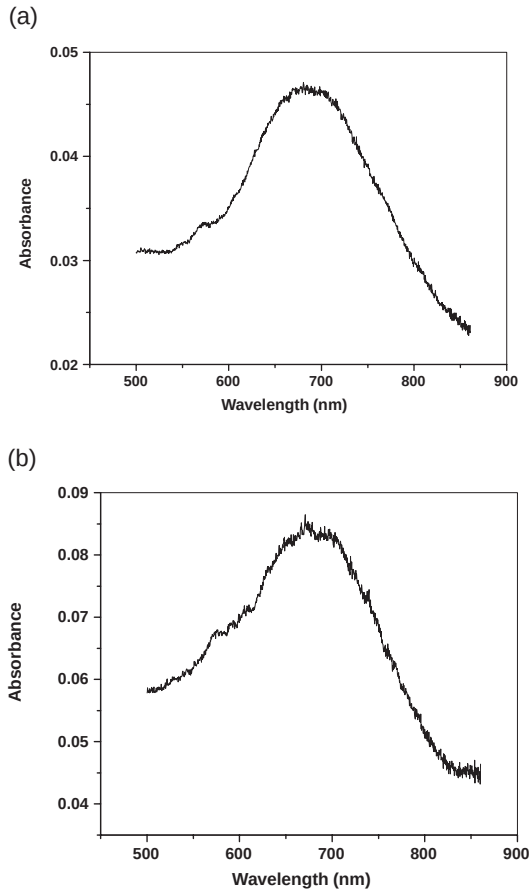

Fig. 4. a) Solid state absorption spectra of complex **1**. b) Solid state absorption spectra of complex **2**.

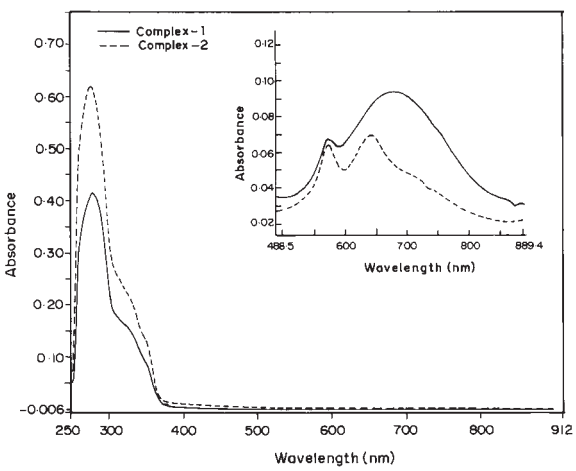

Fig. 5. Absorption spectra of complexes **1** and **2** (10 μM) in dmso with inset showing ligand field transitions (1 mM).

Interaction of Complexes 1 and 2 with DNA. The binding of the metal complexes to DNA was monitored through absorption spectral titration, by monitoring the perturbance in the intraligand transitions at 277 nm and 278 nm for complexes **1** and **2**, respectively. It was found that addition of incremental amounts of DNA resulted in a significant decrease in absorption at 278 nm and a negligible shift in the wavelength. From a plot of $[DNA]/[(\varepsilon_a - \varepsilon_f)]$ versus DNA, the intrinsic binding

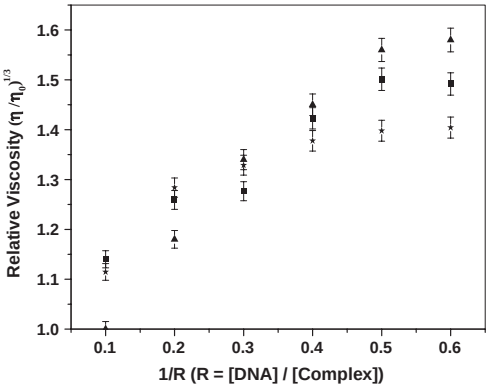

Fig. 6. Effect of increasing amounts of complexes **1** (■), **2** (★), and ethidium bromide (▲) on the relative viscosity of CT DNA at 25 ± 1 °C.

constants were calculated for complexes **1** and **2**, and found to be $(8.4 \pm 0.2) \times 10^3$ and $(10.9 \pm 0.2) \times 10^4$ M^{-1} respectively. The moderate binding for these complexes is comparable to those reported for some intercalators, like AQS (0.35×10^4 M^{-1}) and $[Ru(NH_3)_4DPPZ]^{2+}$ (1×10^5 M^{-1}).[49,50] The classical intercalators, however, show much higher binding constants on the order of 1×10^7 M^{-1}.

Viscosity studies are the least ambiguous and most critical tests to determine the mode of the binding of a metal complex to DNA. While intercalating agents elongate the double helix, leading to an increase in the viscosity, a non-intercalative mode of binding is expected to produce no change, or a decrease in the viscosity of DNA. The variation of the relative viscosity with the addition of increasing concentrations of the two complexes as well as ethidium bromide is given in Fig. 6. Both complexes **1** and **2** show a steady increase in viscosity with an increase in concentration, which is typical of an intercalative mode in the binding of the complex to DNA.

In order to ascertain the ability of **1** and **2** to function as metallonucleases, DNA cleavage was monitored by gel electrophoresis conducted on plasmid pBR322 DNA with complexes **1** and **2**. The naturally occurring supercoiled form (Form I), when nicked, gave rise to an open circular relaxed form (Form II) and upon further cleavage, resulted in the linear form (Form III). When subjected to gel electrophoresis, relatively fast migration was observed for Form I. Form II migrated slowly and Form III migrated between Form I and II. Figure 7 shows the electrophoretic pattern of plasmid DNA treated with complexes (**1**) and (**2**). Control experiments suggest that untreated DNA and DNA incubated with either complex or peroxide alone did not show any significant DNA cleavage (lanes 1, 2, 3, and 4). However, in the presence of peroxide, complexes **1** and **2** were found to exhibit nuclease activity (lanes 5 and 6). This nuclease activity of **1** and **2** could be enhanced by increasing the concentration of H_2O_2, as evident from lanes 7 and 8 in Fig. 7. Nuclease activity exhibited by certain Cu(II) complexes in the presence of hydrogen peroxide was previously attributed to the participation of hydroxyl radical in DNA cleavage.[51] The addition of ethanol to the reaction mixture before electrophoresis was found to suppress the DNA cleaving ability of the complexes (lane 9). This conclusively shows the involvement of the hydroxyl radical in the

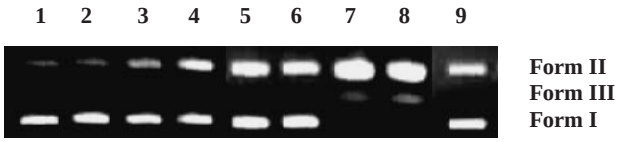

Fig. 7. Cleavage of pBR322 DNA by complexes **1** and **2** in the presence of peroxide. DNA (120 ng) was incubated with **1** and **2** for 1 h in Tris buffer (pH 7.5). Lane 1, DNA control; lane 2, DNA + **1** (75 μM) alone; lane 3, DNA + **2** (75 μM) alone; lane 4, DNA + peroxide (125 μM) alone; lane 5, DNA + **1** (75 μM) + peroxide (125 μM); lane 6, DNA + **2** (75 μM) + peroxide (300 μM); lane 7, DNA + **2** (75 μM) + peroxide (500 μM); lane 8, DNA + **1** (75 μM) + peroxide (500 μM); lane 9, DNA + **1** (75 μM) + peroxide (500 μM) + ethanol (1 M).

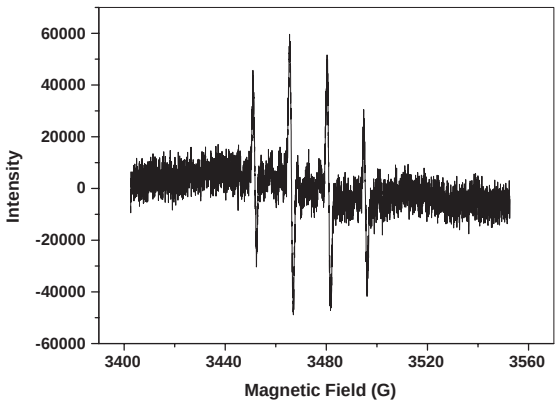

Fig. 8. EPR spectrum of the reaction mixture containing **1** (75 μM), H_2O_2 (125 μM), and DMPO (200 mM).

observed nuclease activity of complexes **1** and **2** in the presence of peroxide. The formation of a hydroxyl radical has also been confirmed through spin-trap experiments. The EPR spectra of complexes **1** and **2** in the presence of H_2O_2 and the spin-trap DMPO shows a typical four-line spectrum ($a_N = 14.85$ G and $a_H = 14.85$ G) attributable to the DMPO-hydroxyl radical adduct (Fig. 8).

It may be relevant to note that many copper(I) and copper(II) phenanthroline complexes have previously been shown to bring about DNA cleavage in the presence of peroxide. Most of these complexes bring about DNA cleavage when used in the 30–100 μM concentration range.[52] Complexes **1** and **2** also bring about DNA cleavage when used in the micromolar concentration range, indicating their potential application as metallonucleases.

Conclusion

p-Tolylterpyridine and *p*-bromophenyl terpyridine ligands form six-coordinate complexes with Cu(II) having a CuN_6 core structure. The crystal structure of the Cu(II) complex of tolyl terpyridine reveals that the complex, unlike most other six coordinate Cu(II) complexes, exhibits axial compression. A Jahn–Teller distortion leading to axial compression is generally associated with the d_{z^2} ground state. Copper(II) complexes of ttpy and Brphtpy, however, have a $d_{x^2-y^2}$ ground state with $g_\parallel > g_\perp$. Hence, it is evident that in these two complexes, the

axial compression results due to the constraints of the ligand. Both of the complexes bind to CT DNA intercalatively with a slight difference in the order of magnitude in their binding constants. Both of these complexes have been shown to nick plasmid DNA in the presence of H_2O_2.

The authors thank CDRI, Lucknow for providing FAB-Mass spectra for the complexes. One of the authors (V.G.V.) acknowledges CSIR for a research fellowship.

References

1 W. Szczepanik, J. Ciesiolka, J. Wrzesiński, J. Skala, and M. Jezowska-Bojczuk, *Dalton Trans.*, **2003**, 1488.

2 C. B. Klein, K. Frenkel, and M. Costa, *Chem. Res. Toxicol.*, **4**, 592 (1991).

3 K. S. Kasprzak, *Chem. Res. Toxicol.*, **4**, 605 (1991).

4 R. Vijayalakshmi, M. Kanthimathi, V. Subramaniam, and B. U. Nair, *Biochim. Biophys. Acta*, **1475**, 157 (2000).

5 B. H. Geierstanger, M. Marksich, P. B. Dervan, and D. E. Wemmer, *Science*, **266**, 646 (1994).

6 C. Liu, J. Zhou, Q. Li, L. Wang, Z. Liao, and H. Xu, *J. Inorg. Biochem.*, **75**, 233 (1999).

7 G. Prativiel, J. Bernadou, and B. Meunier, *Angew. Chem., Int. Ed. Engl.*, **34**, 746 (1995).

8 P. B. Dervan, *Science*, **232**, 464 (1986).

9 A. S. Bouterin, V. Vlassov, S. A. Kazakov, I. V. Kutiavin, and M. A. Podyminogin, *FEBS Lett.*, **172**, 43 (1984).

10 C. OhUigin, D. J. McConnell, J. M. Kelly, and W. J. M. Van Der Putten, *Nucleic Acids Res.*, **15**, 7411 (1987).

11 W. K. Pogozelski, T. J. McNeese, and T. D. Tullius, *J. Am. Chem. Soc.*, **117**, 6428 (1995).

12 P. G. Schultz and P. B. Dervan, *Proc. Natl. Acad. Sci. U.S.A.*, **80**, 6834 (1983).

13 M. W. Van Dyke and P. B. Dervan, *Nucleic Acids Res.*, **11**, 5555 (1983).

14 D. S. Sigman, A. Mazumder, and D. M. Perrin, *Chem. Rev.*, **93**, 2295 (1993).

15 D. S. Sigman, *Acc. Chem. Res.*, **19**, 180 (1986).

16 A. Spassky and D. S. Sigman, *Biochemistry*, **24**, 8050 (1985).

17 "Progress in Inorganic Chemistry: Bioinorganic Chemistry," ed by A. M. Pyle, J. K. Barton, and S. J. Lippard, Wiley, New York (1990), Vol. 38, p. 413.

18 C. J. Burrows and S. E. Rokita, *Acc. Chem. Res.*, **27**, 295 (1994).

19 L. Pearson, C.-H. B. Chen, R. P. Zaynox, and D. S. Sigman, *Nucleic Acids Res.*, **23**, 2255 (1994).

20 J. Stubbe and J. W. Kozarich, *Chem. Rev.*, **87**, 1107 (1987).

21 V. G. Vaidyanathan and B. U. Nair, *J. Inorg. Biochem.*, **93**, 271 (2003).

22 Á. G.-Raso, J. J. Fiol, B. Adrover, V. Moreno, I. Mata, E. Espinosa, and E. Molins, *J. Inorg. Biochem.*, **95**, 77 (2003).

23 X.-L. Wang, H. Chao, H. Li, X.-L. Hong, L.-N. Ji, and X.-Y. Li, *J. Inorg. Biochem.*, **98**, 423 (2004).

24 A. Silvestri, G. Barone, G. Ruisi, M. T. Giudice, and S. Tumminello, *J. Inorg. Biochem.*, **98**, 589 (2004).

25 R. Ren, P. Yang, W. Zheng, and Z. Hua, *Inorg. Chem.*, **39**, 5454 (2000).

26 B. Linkletter and J. Chin, *Angew. Chem., Int. Ed. Engl.*, **34**, 472 (1995).

27 J. K. Barton, "Bioinorganic Chemistry," ed by I. Bertini, H. B. Grey, S. J. Lippard, and J. S. Valentine, University Science Book, Mill Valley (1994), p. 455.

28 K. M. Downey, B. G. Que, and A. G. So, *Biochem. Biophys. Res. Commun.*, **93**, 264 (1980).

29 S. Dhar and A. R. Chakravorty, *Inorg. Chem.*, **42**, 2483 (2003).

30 M. Chikira, Y. Tomizawa, D. Fukita, T. Sugizaki, N. Sugawara, T. Yamazaki, A. Sasano, H. Schindo, M. Palaniandavar, and W. E. Antholine, *J. Inorg. Biochem.*, **89**, 163 (2002).

31 S. Borah, M. M. Melvin, N. Lindquist, and R. A. Manderville, *J. Am. Chem. Soc.*, **120**, 4557 (1998).

32 O. Baudoin, M.-P. Teulade-Fichou, J.-P. Vigneron, and J.-M. Lehn, *Chem. Commun.*, **1998**, 2349.

33 M. Pitie, B. Sudres, and B. Meunier, *Chem. Commun.*, **1998**, 2597.

34 M. A. De Rousch and W. C. Trogler, *Inorg. Chem.*, **29**, 2409 (1990).

35 D. F. Shullenberger, P. D. Eason, and E. C. Long, *J. Am. Chem. Soc.*, **115**, 11038 (1993).

36 a) S. Hashimoto, R. Yamashita, and Y. Nakamura, *Chem. Lett.*, **1992**, 1639. b) S. Hashimoto and Y. Nakamura, *J. Chem. Soc., Chem. Commun.*, **1995**, 1413.

37 K. O. A. Chin and J. R. Morrow, *Inorg. Chem.*, **33**, 5036 (1994).

38 J. Marmur, *J. Mol. Biol.*, **3**, 208 (1961).

39 R. E. Reichmann, S. A. Rice, C. A. Thomas, and P. J. Doty, *J. Am. Chem. Soc.*, **76**, 3047 (1954).

40 J.-P. Collin, S. Guillerez, J.-P. Sauvage, F. Barigelletti, L. De Cola, L. Flamigni, and V. Balzani, *Inorg. Chem.*, **30**, 4230 (1991).

41 W. Spahni and G. Calzaferri, *Helv. Chim. Acta*, **67**, 450 (1984).

42 G. Cohen and H. Eisenberg, *Biopolymers*, **8**, 45 (1969).

43 G. D. Storrier, S. B. Colbran, and D. C. Craig, *J. Chem. Soc., Dalton Trans.*, **1997**, 3011.

44 M. Duggan, B. J. Hathaway, and J. Mullane, *J. Chem. Soc., Dalton Trans.*, **1980**, 690.

45 M. A. Leech, N. K. Solanki, M. A. Halcrow, J. A. K. Howard, and S. Dahaoui, *Chem. Commun.*, **1999**, 2245.

46 C. J. Ballhausen, "Introduction to Ligand Field Theory," McGraw-Hill, NY (1962), p. 134.

47 J. V. Folgado, W. Henke, R. Allmann, H. Stratemeier, D. Beltran-Porter, T. Rojo, and D. Reinen, *Inorg. Chem.*, **29**, 2035 (1990).

48 A. A. El-Bindery and A. Z. El-Sonbati, *Pol. J. Chem.*, **74**, 615 (2000).

49 D. T. Breslin, C. Yu, D. Ly, and G. B. Schuster, *Biochemistry*, **36**, 10463 (1997).

50 R. B. Nair, E. S. Teng, S. L. Kirkland, and C. J. Murphy, *Inorg. Chem.*, **37**, 139 (1998).

51 A. Sreedhara and J. A. Cowan, *Chem. Commun.*, **1998**, 1737.

52 T. Gupta, S. Dhar, M. Netaji, and A. R. Chakravarty, *Dalton Trans.*, **2004**, 1896.